

# Quantum-based Variational Approach for Solving Graph Isomorphism Problems

Yukun Wang<sup>1,2,\*</sup>, Yingtong Shen<sup>1,2,†</sup>, Zhichao Zhang<sup>3</sup>, and Linchun Wan<sup>4</sup>

<sup>1</sup> *Beijing Key Laboratory of Petroleum Data Mining,  
China University of Petroleum, Beijing 102249, China*

<sup>2</sup> *State Key Lab of Processors, Institute of Computing Technology, CAS, Beijing 100190, China*

<sup>3</sup> *School of Mathematics and Physics, University of Science and Technology Beijing, Beijing 100083, China and*

<sup>4</sup> *School of Computer and Information Science, Southwest University, Chongqing 400715, China*

(Dated: March 12, 2025)

The graph isomorphism problem remains a fundamental challenge in computer science, driving the search for efficient decision algorithms. Due to its ambiguous computational complexity, heuristic approaches such as simulated annealing are frequently used to explore the solution space selectively. These methods often achieve high probabilities of identifying solutions quickly, avoiding the exhaustive enumeration required by exact algorithms. However, traditional simulated annealing usually struggles with low sampling efficiency and reduced solution-finding probability in complex or large graph problems. In this study, we integrate the principles of quantum technology to address the graph isomorphism problem. By mapping the solution space to a quantum many-body system, we developed a parameterized model for variational simulated annealing. This approach emphasizes the regions of the solution space that are most likely to contain the optimal solution, thereby enhancing the search accuracy. Artificial neural networks were utilized to parameterize the quantum many-body system, leveraging their capacity for efficient function approximation to perform accurate sampling in the intricate energy landscapes of large graph problems.

**Usage:** Secondary publications and information retrieval purposes.

## I. INTRODUCTION

The graph isomorphism problem is a cornerstone of graph theory and can be reformulated as a classic combinatorial optimization challenge. This problem has garnered substantial attention in theoretical research due to its broad applicability across various domains. For instance, it plays a crucial role in pattern recognition within data analysis [1], the study of molecular crystal structures in chemical engineering [2], and cryptographic protocols aimed at ensuring communication security [3]. As a significant problem in theoretical computer science, the essence of the graph isomorphism problem lies in determining whether two given graphs can be transformed into each other by relabeling their nodes while preserving their structure [4].

The origins of the graph isomorphism problem trace back to the 1950s, when it first emerged in chemistry, where it was used to determine whether two molecular structures were isomorphic by comparing their respective graphs [5]. This application laid the foundation for the theoretical development of graph isomorphism in graph theory. In the 1970s, it gained attention in computer science, with early work focusing on efficient algorithms for specific graph classes and exploring its computational complexity [6]. In the 1980s, Luks[7] introduced decomposition-based algorithms, improving the efficiency of solving graph isomorphism for certain graph types. A major breakthrough came in 2015, when Babai

developed an algorithm that solved graph isomorphism in quasi-polynomial time [8]. Despite this progress, the classification of the problem as complete in P or NP remains unresolved, leaving it an open question in theoretical computer science [7].

The inherent complexity of the graph isomorphism problem makes it challenging to efficiently and accurately determine correct mappings, particularly for large-scale or structurally complex graphs. To address this issue, various methods have been developed in addition to the methods mentioned above, including tree search and backtracking techniques [9], tree-based recursive decomposition and decision tree-based algorithms [10], and VF series algorithms that incrementally match vertex pairs [11, 12]. These classic graph isomorphism algorithms often incorporate a heuristic strategy such as searching for the minimum of an energy function, where the energy function is typically based on differences in vertex and edge correspondences. By combining empirical rules such as vertex neighborhood, degree sequence, and sub-graph structure, these methods prioritize solutions that are closer to meeting the rules, thus narrowing the search space and providing faster approximate solutions. The Simulated Annealing Algorithm (SA) [13–16], inspired by thermodynamic processes, is one such approach that utilizes clever encoding and heuristics to effectively solve graph isomorphism problems. However, SA faces limitations when the optimization landscape is rugged or contains multiple local extrema, resulting in slow and inefficient sampling. These challenges make SA less practical for large-scale graph isomorphism and complex optimization tasks, necessitating the exploration of new algorithms.

Quantum computing, with its inherent parallelism,

\* [wykun06@gmail.com](mailto:wykun06@gmail.com)

† [yingtong0409@163.com](mailto:yingtong0409@163.com)

presents a potential advantage in solving the graph isomorphism problem. Quantum algorithms such as quantum walks, quantum annealing, and the Quantum Approximate Optimization Algorithm (QAOA) use quantum principles to achieve this. Quantum walks capture structural features of graphs through probabilistic transitions between vertices, leveraging quantum interference and superposition principles to enable rapid vertex matching [17–21]. Unlike classical algorithms that rely on step-by-step comparisons or local structure analysis, quantum walks encode graph connectivity into node probability amplitudes, offering a more intuitive graph representation. Using qubits as basic units, they can store far more information than classical bits and significantly reduce the resource overhead for storing graph structure. Quantum annealing transforms the graph isomorphism problem into a quadratic unconstrained binary optimization (QUBO) problem, which is mapped to the Ising spin glass model [22–24]. The ground-state solution can be derived by constructing the corresponding Hamiltonian, providing a potential advantage in optimization. Quantum devices such as the D-Wave quantum annealer have already brought these algorithms into reality [25–28]. QAOA utilizes discrete parameterized quantum circuits combined with classical optimization methods to dynamically adjust parameters. Similar to quantum annealing, it can solve Ising model problems. The key difference lies in that, in such classical-quantum hybrid algorithms, quantum state superposition and entanglement may enable the simultaneous exploration of multiple possible isomorphic mappings. Meanwhile, the classical optimizer adjusts the parameters to find the optimal solution. The combination of these two approaches provides a more effective way to solve the graph isomorphism problem. In addition to these algorithms, some quantum methods focus on encoding graph structures in quantum states to determine graph isomorphism by extracting graph invariants [25, 29, 30]. However, these approaches provide only the necessary conditions for isomorphism without delivering detailed vertex correspondences.

Despite the potential advantages of quantum algorithms for graph isomorphism, challenges remain. Currently, quantum computing operates in the noisy intermediate-scale quantum (NISQ) era, where quantum noise affects the performance of even theoretically mature quantum technologies. These algorithms face hardware limitations such as limited qubit number, quality, connectivity, and gate fidelity. Additionally, quantum annealing algorithms struggle to accurately generate and adjust Hamiltonian parameters for large-scale problems, and environmental interference causes decoherence, threatening the precision and reliability of the algorithms. This restricts the practical implementation of quantum algorithms for graph isomorphism problems. Furthermore, existing quantum algorithms have their own issues. Quantum walks, for example, can be hindered by the regularity of the graph structure, particularly for strongly regular graphs. Quantum annealing re-

quires strict adherence to the adiabatic condition, which is difficult to achieve for large-scale graphs due to complex Hamiltonian structures and small energy gaps. Although NISQ devices hinder the full potential of quantum computing [31], they can still enhance classical algorithms by simulating quantum principles. This has led to the rise of hybrid quantum-classical algorithms [32–36], integrating classical machine learning models with quantum computing, which has become a key area of research. One notable approach is Simulated Quantum Annealing (SQA) [33, 34, 37], a quantum-inspired classical algorithm. When solving the graph isomorphism problem, SQA uses the Path Integral Monte Carlo (PIMC) method [38–41] to map the quantum Hamiltonian onto a classical system, this is achieved by representing the quantum Hamiltonian as the average of multiple classical replica systems through Trotter decomposition, forming "Trotter slices". The SQA method simulates quantum tunneling effects through the path integral Trotter expansion, allowing a higher probability of escaping local optima. It then employs the Metropolis-Hastings method for sampling and optimization.

At each step of the PIMC method, a new spin configuration is proposed randomly. The acceptance of this new configuration is determined by the Metropolis-Hastings algorithm, which compares the energy difference between the current and proposed states. If the new state has lower energy, it is always accepted; if it has higher energy, it is accepted with a certain probability related to the temperature and energy difference. Through multiple iterations of such sampling steps, SQA searches for the optimal solution.

However, similar to traditional SA, SQA has a probability of being trapped in local optima due to the complexity of the energy landscape. While SQA utilizes quantum fluctuations to adjust the search process and has some ability to escape local optima, it does not alter the original energy landscape. The search remains rooted in the intrinsic energy properties. Our algorithm significantly reduces the likelihood of getting trapped in local optima during the search process by creating a more effective "virtual landscape" for searching and employing a parameterized model to guide the search and improve the landscape.

In this work, we propose a quantum machine learning-based heuristic algorithm to effectively solve the graph isomorphism problem using a neural network quantum state (NQS) model. Drawing from the concept of NQS, commonly applied in quantum many-body physics, our method simulates complex quantum systems on classical computers. NQS has gained significant attention in quantum mechanics for solving quantum problems such as ground states and dynamic evolution of quantum systems, as well as quantum tomography [13, 42]. NQS has gained significant attention for addressing quantum problems [43]. This model is often used to solve the ground state and dynamic evolution of quantum many-body systems [44], as well as quantum tomography [45]. Our ap-

proach constructs a quantum multi-body system that encodes a graph structure mapping relationship, enabling dynamic adjustments to the solution space throughout the simulation process. This continuous optimization increases the likelihood of finding the target solution with each sampling. By replacing classical annealing with a parameterized neural network model, we effectively address the dimensionality problem, making it easier to approximate complex quantum systems that traditional methods struggle with.

Starting from the principles of physics, this method constructs a quantum multi-body system containing a graph structure mapping relationship, so that the distribution of the solution space can be continuously adjusted in the process of simulating the evolutionary physical system on a classical computer, thereby continuously improving the probability of hitting the target solution in each sampling process. By replacing classical annealing with a parameterized neural network model, we effectively address the dimensionality problem, optimization is performed based on the "probability landscape" defined by a parameterized Restricted Boltzmann machine, making the search process more efficient and precise. Our method outperforms the SA and SQA algorithms in both sampling efficiency and solution quality, converging to the optimal solution more quickly and accurately. By simulating a quantum multi-body system on a classical computer, the solution space is dynamically adjusted, increasing the probability of hitting the target solution with each sampling. This improvement stems from the fact that our method no longer conducts a blind search on the original energy landscape. Instead, it leverages an RBM to define a probability distribution via a parameterized neural network, forming a dynamic "probability landscape" that is continuously refined during sampling and optimization. As a result, the search trajectory gradually converges toward high-probability regions, corresponding to better solutions. In contrast, SA and SQA methods operate on a fixed energy landscape and rely solely on dynamical evolution to escape local optima, making it more challenging to efficiently locate optimal solutions in high-dimensional and complex energy landscapes. In this sense, it changes the way and path of searching in the solution space, making the search process more targeted and efficient. Therefore, this method not only improves solution efficiency but also effectively mitigates the computational challenges posed by high-dimensional search spaces, providing a more competitive solution for complex optimization problems.

This paper is organized as follows. Section 2 introduces the definition of graph isomorphism problem and maps it to the QUBO problem and the Ising optimization problem[46, 47]. Then, in Section 3 we explain the methods and technical details to solve the graph isomorphism problem. Then, Section 4 shows the performance and experimental results of our algorithm on graph instances, and compares the performance with traditional annealing algorithms and some necessary numerical anal-

ysis. Finally, in Section 5, we think about the theoretical significance of the algorithm proposed in this paper and the future direction of research.

## II. PRELIMINARIES

### A. QUBO Formulation for the Graph Isomorphism Problem

The graph isomorphism problem is a fundamental question in graph theory, involving the possibility of relabeling a graph's vertices to make it structurally identical to another graph. For two graphs  $G_1$  and  $G_2$  to be isomorphic, they must satisfy two fundamental constraints: the vertex correspondence constraint and the edge invariant constraint. The vertex correspondence constraint means that there exists a one-to-one mapping between the vertex set  $V_1$  of graph  $G_1$  and the vertex set  $V_2$  of graph  $G_2$ . The edge invariant constraint requires that for every edge in  $G_1$ , there is a corresponding edge in  $G_2$ , and the structure of the graph remains unchanged according to the mapping between the vertices. In this context, we assume that the graphs under discussion are simple undirected graphs without multiple edges or self-loops unless otherwise specified. The key to solving the graph isomorphism problem is to find a mapping between the two sets of vertices that satisfies both the vertex correspondence and edge invariant constraints. From the perspective of the adjacency matrix, if  $A_1$  and  $A_2$  represent the adjacency matrices of graphs  $G_1$  and  $G_2$ , respectively, then for the graphs to be isomorphic, the vertex mapping that satisfies the two constraints must correspond to a specific permutation matrix  $P$ :

$$PA_1P^{-1} = A_2. \quad (1)$$

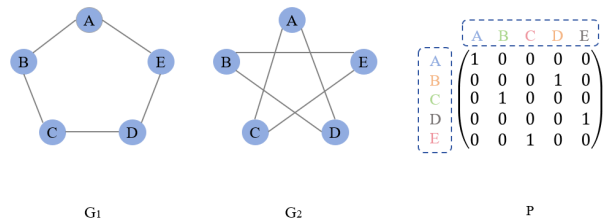


FIG. 1. 5-vertex isomorphic graph instance. The matrix  $P$  that reflects the mapping relationship between graphs  $G_1$  and  $G_2$ .  $P$  is constructed by numbering each vertex and associating each row and column with a node. 1 is entered into the position that correctly corresponds to the vertex, and 0 is entered into the rest.

As illustrated in Fig.1, graphs  $G_1$  and  $G_2$  are isomorphic, by mapping  $\{A, B, C, D, E\}$  in  $G_1$  to  $\{A, C, E, B, D\}$  in  $G_2$ . The vertex mapping is encoded in the matrix  $P$ . To transfer the isomorphic problem

into a QUBO problem, we then transfer the permutation matrix  $P$  into a one-dimensional solution vector:

$$\vec{x} = [x_{AA}, x_{AB}, x_{AC}, x_{AD}, x_{AE}, x_{BA}, x_{BB}, x_{BC}, x_{BD}, x_{BE}, x_{CA}, x_{CB}, x_{CC}, x_{CD}, x_{CE}, x_{DA}, x_{DB}, x_{DC}, x_{DD}, x_{DE}, x_{EA}, x_{EB}, x_{EC}, x_{ED}, x_{EE}], \quad (2)$$

where each component  $x_{ij} (i \in V_1, j \in V_2)$  is either 0 or 1, depending on the mapping relationship.

However, in practice, many graph isomorphism problems involve non-regular graphs. Thus, the one-dimensional solution vector  $\vec{x}$  can be further optimized. As pointed out by [48] if the degree sequences of two graphs differ, they cannot be isomorphic. When the degree sequences are the same, a mapping can only exist between vertices with identical degrees. This property allows for further reduction of the solution space.

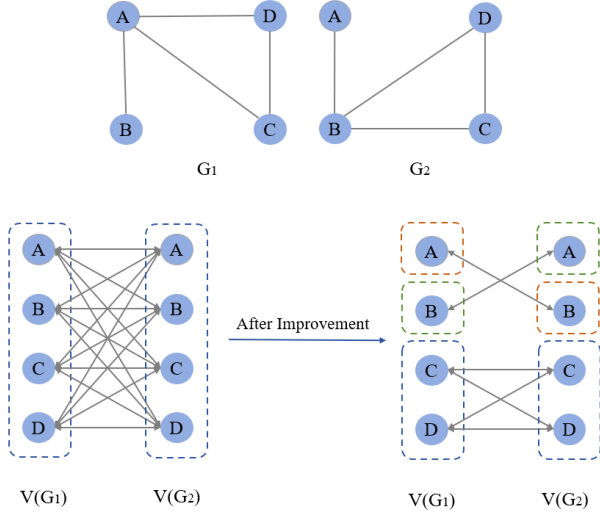


FIG. 2. Ordinary four-vertex isomorphic graphs. The improved encoding method can shorten the length of the solution vector in some non-regular cases.

To illustrate this, consider Fig. 2, where graphs  $G_1$  and  $G_2$  have the same degree sequence  $\{1, 2, 3, 3\}$ . The vertex set can be divided into three smaller subsets, with only vertices of the same degree eligible for mapping to each other. This reduces the solution vector length from 16 to 6, as only the following mappings are possible:  $B$  to  $A$ ,  $\{A, C\}$  to  $\{B, D\}$ ,  $D$  to  $C$ . Thus there has  $\vec{x} = [x_{AA}, x_{AB}, x_{AD}, x_{BA}, x_{CB}, x_{CD}, x_{DC}]$ . This optimization significantly reduces the solution space and makes the isomorphism problem more tractable.

After encoding the solution space into the vector  $\vec{x}$ , the graph isomorphism problem can then be reformulated as a QUBO problem by defining an objective function  $F(\vec{x})$  to be minimized:

$$\min_{x_i \in \{0,1\}} F(\vec{x}) = \vec{x}^T Q \vec{x}, \quad (3)$$

where  $Q$  is a symmetric matrix related to the problem. The matrix element  $Q_{ii}$  represents the linear coefficient of a single variable in  $\vec{x}$ , while  $Q_{ij}$  represents the quadratic interaction coefficient between two variables.

$\vec{x} = \{x_{ij}\}^{|S|}$  is a binary solution vector of length  $|S|$  and  $x_{ij} \in \{0, 1\}$  represents the mapping relationship between vertices  $i \in V_1$  and  $j \in V_2$ . Let  $S = \{(i, j) | i \in V_1, j \in V_2\}$  be the set of possible vertex mapping pairs, considering the consistency of the node degrees between  $V_1$  and  $V_2$ . The objective function  $F(\vec{x})$  is designed to enforce the two fundamental constraints of graph isomorphism:

$$F(\vec{x}) = F_1(\vec{x}) + F_2(\vec{x}), \quad (4)$$

where

$$F_1(\vec{x}) = \sum_{i \in V_1} (\sum_{(i,j) \in S} x_{ij} - 1)^2 + \sum_{i \in V_2} (\sum_{(i,j) \in S} x_{ij} - 1)^2, \quad (5)$$

and

$$F_2(\vec{x}) = \sum_{(i,j) \in S} \sum_{(k,l) \in S} [x_{ij} x_{kl} (A_{1(i,k)} - A_{2(j,l)})^2]. \quad (6)$$

The first part  $F_1(\vec{x})$  is used to ensure the properties of the permutation matrix corresponding to  $\vec{x}$ , that is, each row and each column has only one element that is 1. This ensures compliance with the vertex correspondence constraint. The second part  $F_2(\vec{x})$  ensures that the mapping relationship complies with the second constraint. The term  $(A_{1(i,k)} - A_{2(j,l)})^2$  ensures that only edges matching in both graphs contribute to minimizing  $F_2(\vec{x})$ . We solve the graph isomorphism problem by minimizing this objective function. Let  $\vec{x}_0$  be the optimal solution finally obtained. If  $F(\vec{x}_0) = 0$ , this implies that  $G_1$  and  $G_2$  are isomorphic. The binary entries of  $\vec{x}_0$  encode the vertex mapping between  $G_1$  and  $G_2$  satisfying both constraints. If  $F(\vec{x}_0) > 0$  the graphs are not isomorphic, as no valid mapping exists that satisfies both constraints simultaneously.

## B. Ising optimization problem

The Ising model originates from the spin system in physics and was originally used to describe the phase transition behavior of ferromagnetic materials [49]. One of the goals of studying the Ising model is to observe the change in the total energy of the system under the interaction of spins and the influence of external magnetic fields. In the Ising model, each atom or spin is assumed to be in one of two states, spin up or spin down. These spins are distributed in a lattice and interact with each other's nearest neighbor spins.

The goal of the Ising optimization problem is to evolve an  $N$  qubit quantum system  $|\psi\rangle$  to the ground state  $|\vec{s}\rangle = |s_0, s_1, \dots, s_{N-1}\rangle$  of the problem Hamiltonian  $\hat{H}$ , so that the system energy value  $\langle \vec{s} | \hat{H} | \vec{s} \rangle$  is minimized. Therefore, the goal of the Ising optimization problem usually coincides with the goal of solving the minimum value of the objective function in the QUBO problem. The difference is that the boolean variables in the QUBO problem correspond to the projection results  $\pm 1$  of the single-bit quantum eigenstates  $|+\rangle$  and  $|-\rangle$  in the quantum Ising model on the Pauli-Z operator. To describe quantum systems, we use the Pauli-Z operator  $\sigma_i^z$  to replace every classical binary variable. The Hamiltonian of the quantum Ising model is generally defined as

$$\hat{H} = - \sum_{i,j=1}^N J_{ij} \sigma_i^z \sigma_j^z - \sum_{i=1}^N h_i \sigma_i^z, \quad (7)$$

where  $J_{ij}$  is the coupling constant describing the spin pair  $\sigma_i^z, \sigma_j^z$ , and  $h_i$  is the effect of the external magnetic field on each spin.

### III. NQS-BASED VARIATIONAL ALGORITHM FOR GRAPH ISOMORPHISM

#### A. Hamiltonian Construction of Graph Isomorphism Problem

According to the definition of the Ising model, for a graph isomorphism instance with a solution vector  $\vec{x}$  of length  $L$ ,  $L$  spin/qubits are used for encoding. The binary variable  $x_{ij}$  is mapped to a spin/qubit  $s_{ij}$  via the Pauli-Z operator, which is used to construct the problem Hamiltonian  $\hat{H}$ . The solution space of the original problem is then mapped to a quantum system  $|\psi\rangle$  of size  $2^L$ , where  $(i, j) \in S$ , the vertex mapping pair set. Therefore, the ground state of  $\hat{H}$  contains vertex mapping relationships, and the corresponding ground state energy  $\lambda$  is an important basis for evaluating whether the mapping relationship is correct. From the two constraints of the graph isomorphism problem, we can see that:

$$\hat{H} = \hat{H}_1 + \hat{H}_2, \quad (8)$$

where

$$\hat{H}_1 = \sum_{i=1}^N \left( \sum_{(i,j) \in S} \frac{\sigma_{ij}^z + I}{2} - I \right)^2 + \sum_{j=1}^N \left( \sum_{(i,j) \in S} \frac{\sigma_{ij}^z + I}{2} - I \right)^2, \quad (9)$$

and

$$\hat{H}_2 = \sum_{(i,j) \in S} \sum_{(k,l) \in S} \frac{1}{4} [(\sigma_{ij}^z \sigma_{kl}^z + \sigma_{ij}^z + \sigma_{kl}^z + I)(A_{1(i,k)} - A_{2(j,l)})^2]. \quad (10)$$

The eigenstate of  $\hat{H}$  correspond to the different configurations of  $x_{ij}$ , where each configuration (with  $x_{ij} \in \{0, 1\}$ ) represents a possible mapping relationship in the graph isomorphism problem, and is denoted as  $|\vec{s}\rangle$ . For any eigenstate  $|\vec{s}\rangle$  in the quantum system, which serves as the quantum representation of a mapping solution to the graph isomorphism problem, the associated energy eigenvalue is defined as follows:

$$\langle \vec{s} | \hat{H} | \vec{s} \rangle = \begin{cases} 0, & \text{the right mapping combination} \\ \lambda, & \text{otherwise} \end{cases} \quad (11)$$

Here,  $\lambda$  records the number of configuration items that violate the constraints of the graph isomorphism mapping. Its value is determined by equations (5) and (6). Initially, the bijection-related objective function in equation (5) is evaluated. Notably, any redundant mapping increases the value of  $F_1(\vec{x})$  by 1. In order to determine the upper bound of  $F_1(\vec{x})$ , it is essential to include the maximum possible number of redundant mappings beyond the valid bijection that satisfies the cost function. Consider two simple undirected graphs,  $G_1$  and  $G_2$  each with  $N$  vertices. Assume that every vertex in  $G_1$  maps to every vertex in  $G_2$ , and each vertex has one correct mapping among the  $N$  mapping relationships, with the remaining mappings being redundant. According to equation (5), this results in a penalty value of  $2N(N-1)^2$ . It is important to note that when traversing the vertices of  $G_1$  and  $G_2$  accounts for  $F_1(\vec{x})$  each redundant mapping twice. Therefore, the upper bound of  $F_1(\vec{x})$  is given by  $2N(N-1)^2$ .

Then, we check the edges mapping objective function  $F_2(\vec{x})$ . Under the condition that  $F_1(\vec{x})$  reaches its maximum value, the length of  $\vec{x}$  is  $N^2$ , implying that both graphs  $G_1$  and  $G_2$  are fully connected. As a result,  $x_{ij} = x_{kl} = 1, \forall (i, j), (k, l) \in S$ . For the term  $(A_{1(i,k)} - A_{2(j,l)})^2$ , the following cases are considered:

$$(A_{1(i,k)} - A_{2(j,l)})^2 = \begin{cases} 0, & \text{if } i \neq k \text{ and } j \neq l, \\ 0, & \text{if } i = k \text{ and } j = l, \\ 1, & \text{others,} \end{cases} \quad (12)$$

when  $i \neq k$  and  $j \neq l$ , means under the mapping  $x_{ij} = x_{kl} = 1$ , the edge invariant constraint. In the case  $i = k$  and  $j = l$ , there is  $A_{1(i,k)} = A_{2(j,l)} = 0$  since there is no cycle in a simple undirected graph. The third case, where  $i = k$  and  $j \neq l$  or  $i \neq k$  and  $j = l$ , the absence of cycles in the graph ensures that  $A_{1(i,k)}$  and  $A_{2(j,l)}$  are not simultaneously zero, resulting in the theoretical maximum value  $2N^2(N-1)$ .  $F_2(\vec{x})$  checks whether the edge relationships are consistent for mapped vertex pairs, incrementing its value by 1 for each violation. However, it does not verify compliance with bijection principles, as this is constrained by  $F_1(\vec{x})$ . Thus, the maximum value of equation (5) is added to the maximum value of equation (6), yielding an upper bound for  $\lambda$  of  $2N^2(N-1) + 2N(N-1)^2$ .

## B. Neural Network Quantum States Approximate Wavefunctions

Above, we have encoded the graph isomorphism problem into the Hamiltonian  $\hat{H}$ , where the lowest energy state of  $\hat{H}$  captures the isomorphism information of the graph. In principle, we could continue to exploit quantum advantages through methods such as quantum annealing, QAOA, or quantum walks to solve the problem. However, considering the current limitations of practical quantum devices, algorithms that employ quantum-inspired classical simulations can also offer advantages. Therefore, we focus on applying quantum-inspired approaches to solve the problem via classical simulation. While the SQA algorithm has been widely researched, it has certain limitations. To address these issues, we use NQS to represent the solution space. We then apply the quantum Monte Carlo method to estimate the ground state energy as accurately as possible, which helps solve these challenges.

NQS is an innovative method for representing quantum states [43, 50], widely used in quantum computing and quantum physics. In quantum physics, the many-body problem refers to describe the behavior of a system composed of a large number of interacting particles. The wave function of such a system has exponential complexity because the interaction between each particle and all other particles needs to be considered [51, 52]. This results in analytical difficulties in describing and solving the wave function for complex quantum systems. Following the research of [43], the strong expressiveness of neural network models in machine learning provides an approximate solution to this problem, which has also greatly promoted the research progress of condensed matter physics [53–57].

In this work, we first choose the more flexible and simpler neural network model, the Restricted Boltzmann Machine (RBM), to parameterize the quantum system's wave function. In theory, the wave function of a many-body quantum system requires an exponential amount of data to fully encode. However, in practical applications, we hope to select a suitable representation method to appropriately simplify the wave function of the system related to the problem, and the graph model is good at this. Then we perform the quantum Monte Carlo method to obtain the ground state energy as accurately as possible. Of course, the ultimate goal of the graph isomorphism problem is not only to obtain the energy value, which serves as the basis for determining whether two graphs are isomorphic, but also to increase the probability that the target candidate mapping solution is measured by evolving the system to the ground state. In our work, the measurement process for simulating the quantum system is replaced by sampling.

RBM is a two-layer bipartite graph [58], typically consisting of two types of units: hidden layer units and visible layer units. RBM use hidden units to model high-order and non-linear patterns in data, enhancing

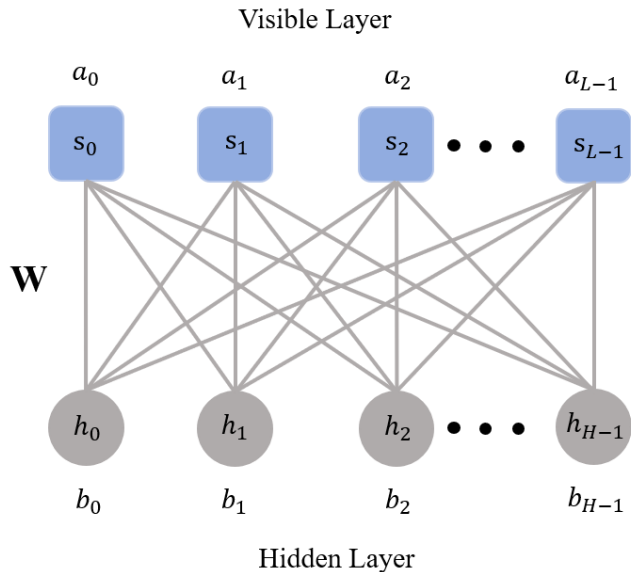


FIG. 3. Structure of a Restricted Boltzmann Machine.

the capability to represent wave functions [59]. The structure of the model is shown in Fig.3. For a solution vector  $\vec{x}$  of length  $L$  in the graph isomorphic problem, the corresponding quantum eigenstate is defined as  $|\vec{s}\rangle = |s_i\rangle^{\otimes L}$ , which is used as input to interact with the bias vector  $\vec{a} = \{a_i\}$  in the visible layer. This input is fully connected to the hidden layer containing  $H$  binary hidden nodes. The bias vector of the hidden layer is  $\vec{b} = \{b_j\}$ , where  $s_i, h_j \in \{1, -1\}$ . The connection relationship between each vertex in the two layers is determined by the corresponding connection weight parameter  $W = \{W_{ij}\}$ . The complete set of parameters for the RBM model is given by  $\Omega = \{\vec{a}, \vec{b}, W\}$ , where  $\Omega_i \in R$ . Thus, the wave function of the quantum system can be expressed as:

$$\psi(\vec{s}, \Omega) = \sum_{\vec{h}} e^{\sum_i s_i a_i + \sum_{ij} s_i W_{ij} h_j + \sum_j h_j b_j} \quad (13)$$

Given that the units in the RBM layers are not connected within their respective layers, we can simplify this expression to:

$$\psi(\vec{s}, \Omega) = e^{\sum_i a_i s_i} \prod_j 2 \cosh(b_j + \sum_i W_{ij} s_i) \quad (14)$$

Therefore, after mapping the solution space of the graph isomorphism problem to the quantum system, the corresponding neural network quantum state [60] can be written as:

$$|\psi\rangle = \sum_{\vec{s}} \psi(\vec{s}, \Omega) |\vec{s}\rangle \quad (15)$$

Now, to calculate the expectation value of the Hamiltonian  $\hat{H}$ , we use,

$$\langle \psi(\vec{s}, \Omega) | \hat{H} | \psi(\vec{s}, \Omega) \rangle = |\psi(\vec{s}, \Omega)|^2 \lambda = P(\vec{s}) \lambda \quad (16)$$

Here,  $|\psi(\vec{s}, \Omega)\rangle = \psi(\vec{s}, \Omega) |\vec{s}\rangle$  used to represent the state of non-normalized mapping  $|\vec{s}\rangle$ . Therefore, we realize the parameterized representation of the quantum system through ansatz in equation(14). In quantum mechanics, the eigenstate wave function in the system determines the probability that the eigenstate is observed to some extent, as shown in equation(15). This provides a theoretical foundation for mapping quantum systems into probability distribution space.

Next, we will apply an optimization program to perform variational operations on the system's wave function. The goal is to solve for the ground state of the system and obtain the optimal mapping of the graph vertices.

### C. Variational Solution of Graph Isomorphism Problem using NQS

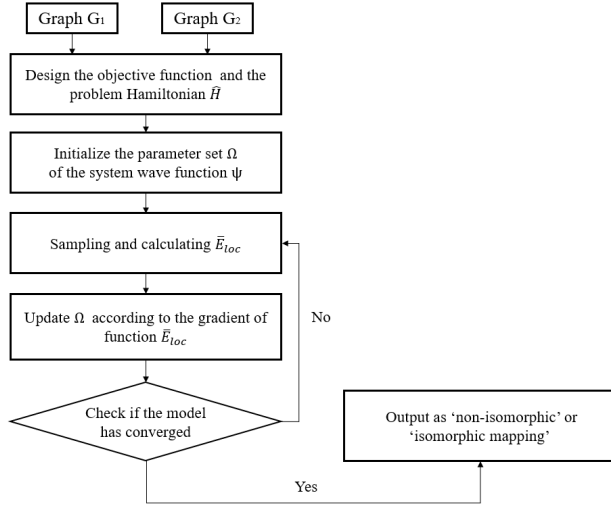


FIG. 4. Proposed NQS-based GI algorithm.

In this work, we integrate the variational wave function obtained from the neural network model into the variational Monte Carlo (VMC) method. By adjusting the energy of the quantum system through Monte Carlo sampling and applying the variational principle, we aim to approximate the ground state and minimize the energy of the system. In detail, for the problem Hamiltonian  $\hat{H}$  of the graph isomorphism problem, the energy of the system represented by the NQS state  $|\psi\rangle$  is given by:

$$E_{global} = \frac{\langle \psi | \hat{H} | \psi \rangle}{\langle \psi | \psi \rangle} \quad (17)$$

This represents the expectation value of the Hamiltonian  $\hat{H}$  with respect to the NQS  $|\psi\rangle$ , providing a measure of the system's energy.

Next, we assume that  $n$  samples  $\{|\vec{s}\rangle\}^n$ , representing a set of eigenstates of  $\hat{H}$ , are collected from the system using the Metropolis-Hastings method. The Metropolis-Hastings algorithm generates a sequence of samples from the target distribution  $P(\vec{s})$  which means the modulus squared distribution of the system's wave function. by constructing a Markov chain. It accepts or rejects new samples based on the relative values of the target probability distribution at the current and proposed states [61].

$$E_{loc} = \sum_{\vec{s}} \langle \psi(\vec{s}, \Omega) | \hat{H} | \psi(\vec{s}, \Omega) \rangle = \sum_{\vec{s}} P(\vec{s}) \lambda \quad (18)$$

$$\bar{E}_{loc} = \frac{1}{M} \sum E_{loc} \approx E_{global} \quad (19)$$

The local energy  $E_{loc}$  is calculated using the sample configuration, repeated  $M$  times, and the overall energy expectation of the system is estimated by the sample energy expectation value  $\bar{E}_{loc}$  (equation(19)). We transform the graph isomorphism problem into the problem of solving the ground state of the quantum system  $\hat{H}$ , meaning that we aim to minimize  $E_{global}$  by continuously adjusting the parameters of the variational wave function. This adjustment ensures that the probability amplitude of the eigenstate  $|\vec{s}\rangle$ , which contains the target solution information, increases gradually. The approximation to the ground state is achieved by tuning the wave function parameters  $\Omega = \{\vec{a}, \vec{b}, W\}$ , corresponding to the variational part of the VMC algorithm. This approach provides a systematic method for approximating the ground state energy and obtaining the optimal mapping for the graph isomorphism problem through the VMC method.

As the scale of the problem solution space increases, the Hilbert space dimension of the quantum system becomes very large. The sampling component of the VMC algorithm helps mitigate this issue by leveraging sampling techniques based on relevant statistical principles [62]. To ensure statistical precision in estimation, the sample size must be large enough. However, increasing the sampling scale significantly increases computational time and memory consumption. Therefore, a balance between computational precision and resource expenditure is maintained to ensure that sufficiently accurate results can be obtained within reasonable computational resource limits. Sampling introduces statistical uncertainty into the algorithm, and according to the zero-variance principle of VMC, when the system's wave function  $|\psi\rangle$  approaches the true ground-state wave function, the expected variance of the sample energy tends to 0. In this case,  $\bar{E}_{loc} = E_{global} = 0$  [63].

Therefore, this is used as an indicator in the experiments to determine whether the system has converged

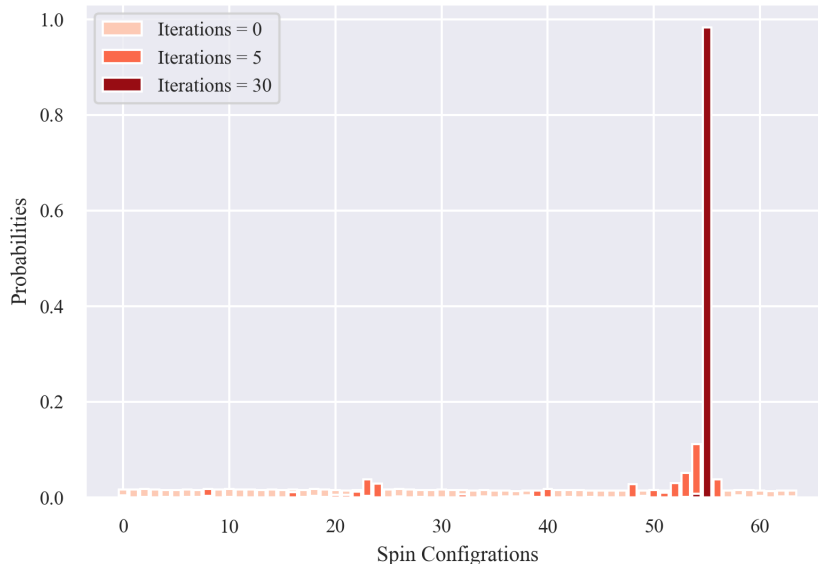


FIG. 5. Schematic figure of the sampling optimization process. It can be seen that the NQS optimization process quickly increases the probability of sampling high-quality solutions (which means producing lower penalty function values), thereby making the target solution stand out.

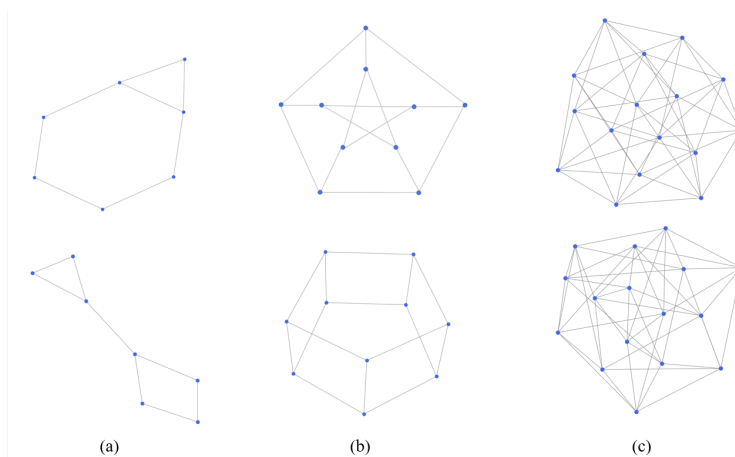


FIG. 6. Three different types of non-isomorphic graph instances, all with the same degree sequence. (a) is a general graph instance with  $N = 7$  vertices, its degree sequence is  $[2, 3, 3, 2, 2, 2, 3]$ . (b) is a regular graph instance with  $N = 10$  vertices, and its degree sequence is  $[3, 3, 3, 3, 3, 3, 3, 3, 3, 3]$ . (c) is a strongly regular graph instance with  $N = 16$  vertices, its degree sequence is  $[6, 6, 6, 6, 6, 6, 6, 6, 6, 6, 6, 6, 6, 6, 6, 6]$ .

to the ground state. When the variance reaches zero, all local energy values become identical, indicating that the system has reached a stable state. Additionally, when the energy expectation of the samples no longer changes with successive sampling and optimization steps, it signifies that the parameter update step size is approaching zero and the model has converged. At this point, the sample expectation value provides the best approximation to the energy of the ground state of the system. This also suggests that, in the probability distribution of the solution space after training, the probability ampli-

tude of the target solution is typically much higher than that of non-target solutions, which leads to a significant improvement in the hit rate of the algorithm once the model converges. Although, in practice, the wave function in the VMC algorithm is usually an approximation and it is challenging to achieve the ideal situation of zero variance, this principle provides an optimization criterion for the algorithm. Meanwhile, reducing the variance of the sample energy expectation and minimizing the energy expectation value work together in the gradient estimation of the variational part of the VMC algorithm,



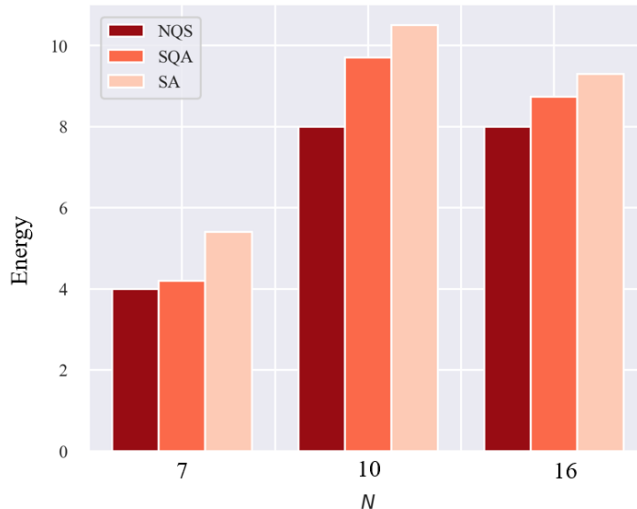


FIG. 7. The average minimum system energy of three algorithms on different types of non-isomorphic graphs.

collaboratively guiding the adjustment of the wave function parameters. This enables a more precise estimation of the true ground state of the system. Fig.4 illustrates the complete process of this algorithm.

We take the 4 vertexes isomorphic graph in Fig.2 as an example to check how the target distribution of samples changes with the optimization of  $\Omega$ . According to the instance encoding shown in Fig.2, the length of the mapping solution vector is 6, resulting in a solution space of size  $2^6$ . The inspection result is Fig.5. The set of initial parameters  $\Omega$  is random initialized from a normal distribution with a mean of 0 and a standard deviation of 0.01 by default.

In the first iteration of the algorithm, the sample solutions obtained correspond to the mapping results such as  $[0, 1, 1, 0, 1, 1]$ ,  $[1, 1, 0, 0, 1, 0]$  and  $[0, 1, 1, 1, 0, 1]$ , among other candidate solutions. Based on these samples, the computed expected energy value is 6.25. The optimization direction is adjusted by minimizing the energy expectation of the samples, and the set of parameters  $\Omega$  is updated using the stochastic gradient descent (SGD) and stochastic reconfiguration (SR) methods, the program repeats this process after each subsequent iteration of sampling. Specifically, the gradient of the energy expectation function  $\bar{E}_{loc}$  with respect to the parameters  $\Omega$  is computed, guiding the optimization process along the negative gradient direction to approach the minimum of the function. Through this iterative optimization process, the system state progressively approaches the target solution, effectively capturing the isomorphism structure of the graph. It is obvious that after 5 rounds of iteration, the sampling will cluster, that is, the probability distribution will gradually concentrate on the target solution area. Consequently, the VMC method directs the sampling toward high-probability regions, which correspond to areas of lower energy. Simultaneously, the algorithm's

variational adjustment of the system parameters causes the sample probability distribution to evolve in the optimization landscape, further guiding the sampling toward the target solution and reducing the probability of being trapped in local optima. After 30 rounds of iteration, the wave function parameters of the system are close to convergence, which is specifically manifested as the probability of the target solution being 0.983, which is close to 1. At this time, sampling can eliminate the interference of the wrong mapping scheme. Finally, a sampling operation is performed on the converged model, yielding the mapping solution  $\vec{x} = [x_{AB}, x_{BA}, x_{CC}, x_{CD}, x_{DC}, x_{DD}]$  obtained is  $[1, 1, 0, 1, 1, 0]$ . This corresponds to the output mapping  $\{A \leftrightarrow B, B \leftrightarrow A, C \leftrightarrow D, D \leftrightarrow C\}$ .

#### IV. NUMERICAL VALIDATION

In this paper, we compare the performance of the NQS and VMC-based algorithm with classical SA and SQA methods in terms of algorithm accuracy and evolution time for solving the graph isomorphism problem. The experimental setup primarily focuses on testing these algorithms on isomorphic graphs, evaluating various performance aspects in determining the correct vertex mapping solutions. Additionally, experiments were conducted on three different types of non-isomorphic graphs to further demonstrate the capability of the NQS and VMC-based algorithm in distinguishing non-isomorphic graphs. Before delving into this comparison, we first introduce the SA and SQA algorithms and their configurations.

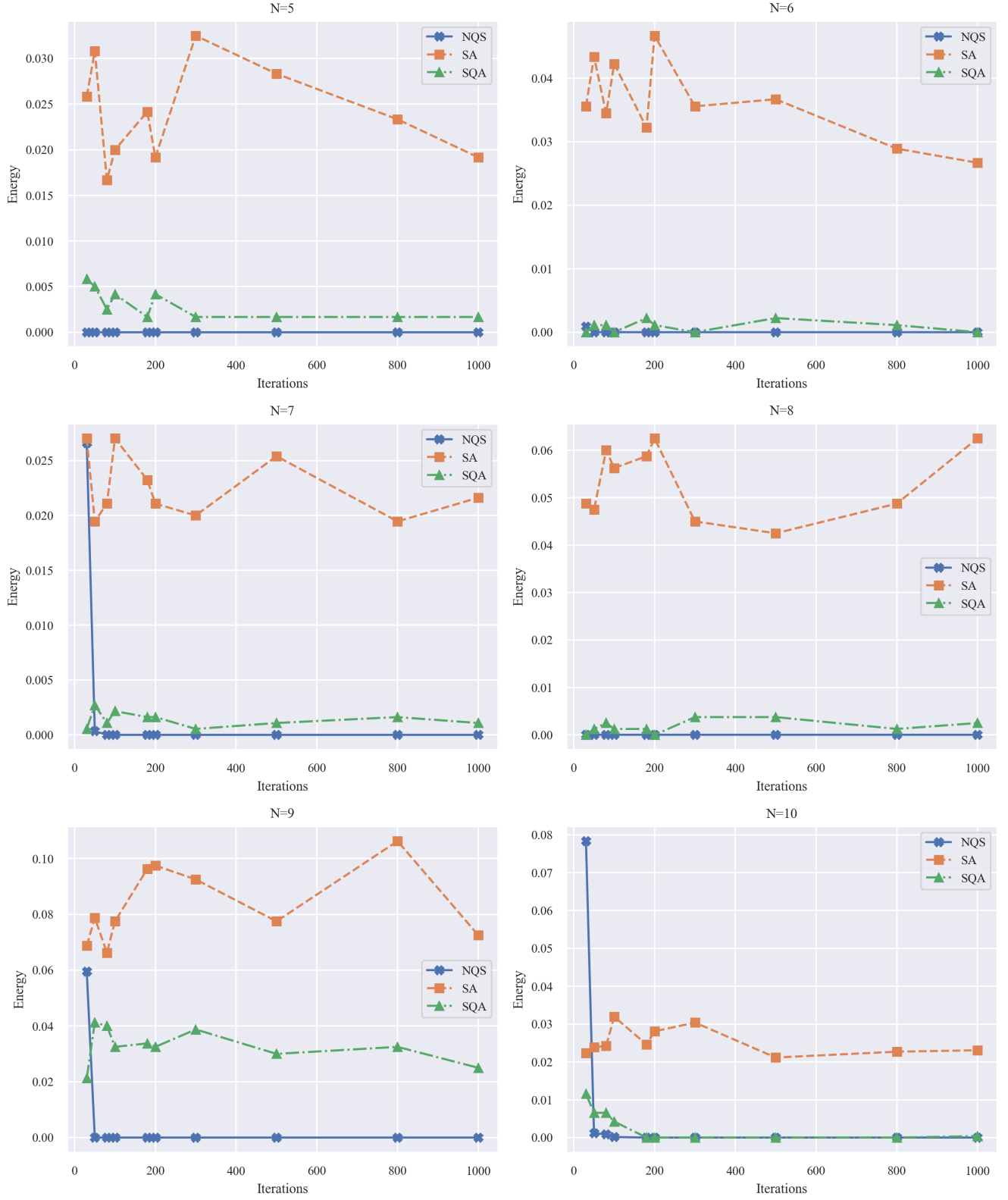


FIG. 8. The figure demonstrates the change in the average residual energy of graph instances with  $N = 5, 6, 7, 8, 9, 10$  as iterations progress. Compared to SA and SQA, the NQS method initially shows higher energy but achieves a more significant reduction through variational optimization and maintains a more stable ground state.

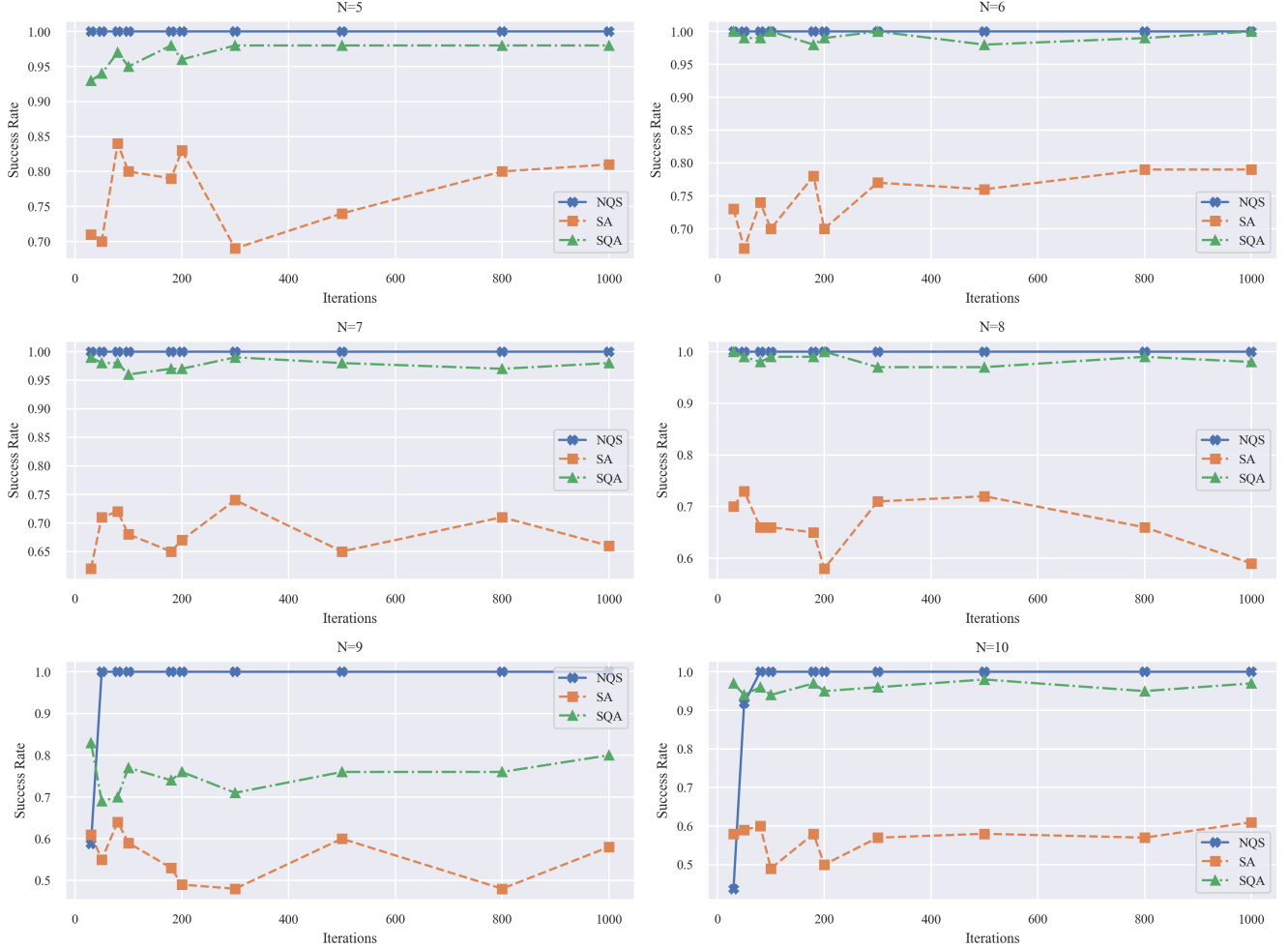


FIG. 9. Line graph showing the hit rate of the three algorithms as the number of iterations changes.

### A. Implementation Details of SA and SQA Algorithms

Simulated annealing employs a random search algorithm where the system begins from a random initial state and explores the solution space by flipping qubits. At high temperatures, the system has a probability of accepting suboptimal solutions, which helps escape from local minima.

As the temperature decreases over time, the probability of accepting such solutions decreases, and the system gradually converges to a stable state to find the optimal solution. As a typical classical heuristic algorithm, SA performance will be compared with the NQS-based algorithm in this paper. To implement the SA algorithm, we follow these steps:

1. Initialization. Start by initializing a solution vector  $\vec{x}_0$ . Set the initial temperature of the system to  $T_0$  and design the objective function  $F$  of the graph isomorphism problem, we will refer to it as the energy function later.

2. Exploring the Solution Space. Select a new solution  $\vec{x}_1$  randomly from the neighborhood of the current solution, which is achieved by flipping a random bit in the solution vector. Compute the energy change  $\delta F = F(\vec{x}_0) - F(\vec{x}_1)$  and update the solution using the Metropolis criterion. If  $\Delta E \leq 0$ , accept the new solution; if  $\Delta E > 0$ , accept it with a probability of  $P(\Delta E, T) = e^{-\Delta E/T}$ . This probabilistic acceptance of non-optimal solutions helps escape local minima. Note that the system temperature remains unchanged in this step. We define  $N_{sweep}$  as the number of solution space explorations at a fixed temperature, where  $N_{sweep}$  new solution vectors are generated by flipping bits.
3. Annealing. Gradually reduce the system temperature according to the set temperature schedule, transitioning from  $T_0$  to  $T_1$ .
4. Repeat the solution space exploration and annealing steps until the system temperature reaches the final value  $T_{final}$ . The number of temperature

drops is denoted by  $N_{annealing}$ , which, together with  $T_0$  and  $T_{final}$ , defines the annealing schedule of the SA algorithm. The process ends when the temperature reaches  $T_{final}$ , outputting the historical optimal solution found during the exploration.

The SQA algorithm, on the other hand, leverages quantum tunneling to efficiently find global optima, guided by system temperature and transverse field strength. Unlike classical simulated annealing, SQA uses quantum tunneling to overcome energy barriers and is implemented here using the PIMC method.

PIMC method is based on imaginary time evolution, which is key to transforming the evolution of quantum systems into thermodynamic equilibrium problems of classical systems[64]. For a given Hamiltonian  $H$ , the imaginary time evolution operator is defined as  $\hat{U}(\beta) = e^{-\beta H}$ , where  $\beta = \frac{1}{T}$  is the inverse of the system temperature. For any initial state  $|\psi_0\rangle$ , the system can evolve toward the ground state  $|\psi_f\rangle$  through imaginary time evolution, satisfying:

$$\lim_{\beta \rightarrow \infty} \hat{U}(\beta)|\psi_0\rangle = |\psi_f\rangle \quad (20)$$

Assuming the ground state energy is  $E_f$ , the ground state  $|\psi_f\rangle$  satisfies the eigenvalue equation:

$$H|\psi_f\rangle = E_f|\psi_f\rangle \quad (21)$$

According to the theory of thermodynamic equilibrium, the probability of a quantum state under temperature  $T$  satisfies:

$$P(|\psi\rangle, T) = \frac{1}{Z} e^{-\beta \langle \psi | H | \psi \rangle} = \frac{1}{Z} \langle \psi | e^{-\beta H} | \psi \rangle = \frac{1}{Z} \langle \psi | \hat{U}(\beta) | \psi \rangle, \quad (22)$$

where  $Z$  is the partition function,  $Z = \sum_{|\psi\rangle} e^{-\beta \langle \psi | H | \psi \rangle}$ . When the system is in thermal equilibrium and the temperature is low, ignoring the degeneracy of the ground state, the probability of the ground state is typically close to 1.

To facilitate the calculation of the imaginary time evolution  $\hat{U}(\beta)|\psi\rangle$ , the Trotter-Suzuki decomposition is commonly employed. This decomposes the imaginary time evolution operator into the product of local operators. In doing so, we map the original problem Hamiltonian into a classical system consisting of  $\tau$  coupled copies of the original system, known as Trotter slices. Taking the Hamiltonian of the Ising model as an example, after mapping, it is

$$H(t) = - \sum_{k=1}^{\tau} \left( \sum_{(i,j)} J_{ij} \sigma_i^k \sigma_j^k + J(t) \sum_{i=1}^N \sigma_i^k \sigma_i^{k+1} \right), \quad (23)$$

where  $\tau$  is the number of Trotter slices,  $\sigma_i^k$  is the  $i$ -th spin on the  $k$ -th slice,  $J(t) = -\frac{\tau T}{2} \ln(\tanh(\frac{\Gamma(t)}{\tau T}))$  is the coupling function between slices, which is the coupling along the imaginary time dimension, and  $J_{ij}$  describes

the coupling in the original two-dimensional direction of the Ising model, where  $\Gamma(t) = \Gamma_0(t-1)$  is a linear function of time, representing the transverse field strength of the quantum system, time  $t \in [0, 1]$ . On this basis, the Metropolis-Hastings Monte Carlo algorithm is used to explore the solution space. Each exploration is called a Monte Carlo Step (MCS), and each MCS consists of one local flip and one global flip.

- Local movement: A randomly selected spin in a single slice is flipped, and the energy difference is calculated. The change is accepted or rejected using the Metropolis-Hastings criterion, allowing the system to escape from local optima.
- Global flip: All spins of the same qubit across all slices are flipped simultaneously, and the new solution is evaluated based on the energy difference.

The SQA algorithm reduces system energy by gradually decreasing the transverse field strength. Similar to SA, it explores the solution space through multiple MCS at each transverse field strength. When  $\Gamma$  decreases from  $\Gamma_0$  to  $\Gamma_{final}$  or the system energy reaches 0, annealing is completed. The slice with the lowest energy is then selected as the result.

In the SA algorithm, the system relies primarily on thermal fluctuations to escape local minima, which means that at high temperatures, the system can accept suboptimal solutions and move through the solution space to explore more potential optimal solutions. As the temperature decreases, the system gradually converges to an (possibly local) optimal solution. Therefore, when the energy function has multiple local minima, SA may get stuck in a local optimum, especially in the complex energy landscape introduced by graph isomorphism problems with intricate structures.

In a quantum system, particles are not always restricted by classical physical potential barriers, but can tunnel through these barriers with a finite probability, a phenomenon known as quantum tunneling. SQA primarily simulates quantum tunneling by controlling the transverse field term. In the early stages, even if a local optimum is surrounded by a potential barrier, the system still has a probability of tunneling into a better solution space, rather than gradually climbing over the energy barrier like in SA. As time progresses, the transverse field strength decreases, and quantum tunneling behavior gradually fades, causing the system's behavior to transition from quantum tunneling to classical optimization, eventually stabilizing at a (possibly local) optimal solution. Although SQA has strong capabilities in avoiding local optima, it still has some limitations: for certain problems, the tunneling rate may be very small, especially when the energy barrier is wide and high, making the algorithm's required long time. Additionally, tunneling may lead to the selection of non-optimal solutions if the optimal solution is surrounded by regions with complex barrier structures, and the system may still tunnel

to a suboptimal solution. Therefore, compared to NQS, SQA does not alter the energy landscape of the solution space; it simply provides a different search strategy that is more effective than SA in avoiding local optima.

NQS parameterizes the quantum system using neural networks, allowing the optimization process to no longer be confined to a fixed classical energy function. Instead, it can variationally optimize the parameters of the wavefunction, enabling NQS to reshape the distribution of the solution space to some extent. By creating more efficient "virtual landscapes" and using parameterized models to guide the search and improve the distribution, the NQS algorithm makes the representation of certain low-energy states more concentrated, thereby optimizing the search process, improving the barrier structure of the landscape, and significantly reducing the probability of getting trapped in local optima. However, SA and SQA do not alter the energy landscape of the objective function itself; the local minima and barriers still exist, but the algorithms use different approaches to cross these barriers.

To compare the three algorithms, we set the exploration count for SQA and SA as  $N_{sweep}$  and the cooling steps as  $N_{annealing}$ . For the NQS method, the sampling scale per round is set to  $N_{sweep}$ , and the optimization iterations to  $N_{annealing}$ . This ensures all algorithms explore the solution space  $N_{annealing} * N_{sweep}$  times, with  $N_{sweep}$  increasing with graph and solution space scales. The purpose of this is to ensure that the three algorithms probe the solution space with the same sampling scale and computational steps, thereby allowing for a more accurate comparison of their performance differences. The initial temperature  $T_0$  of the SA algorithm is set to 100, with a final temperature  $T_{final}$  of 0.667. The initial transverse field strength  $\Gamma_0$  of the SQA algorithm is also set to 100, and the final transverse field strength  $\Gamma_{final}$  is 0.667, maintaining relative consistency with the SA algorithm. For details on the hyperparameter settings of the three algorithms, see Table I.

## B. Non-isomorphic Graph

We tested non-isomorphic graphs using the variational method based on NQS, demonstrating its ability to distinguish them. Since graphs with different degree sequences can be identified as non-isomorphic during preprocessing, the non-isomorphic graphs tested in this section all share the same degree sequence.

We conducted experiments on several types of graphs

(as shown in Fig.6). A graph  $G$  is  $k$  regular if all vertices  $v$  satisfy  $Deg(v) = k$ . For example, in  $N = 10$  vertex graphs, the Petersen graph and the Pentagonal Prism graph are both 3 regular due to their high symmetry and  $Deg(v) = 3$  for all vertices. Strongly regular graphs are classified by parameters  $(N, k, \lambda, \mu)$ , where graphs with identical parameters belong to the same family. Here,  $N$  denotes the number of vertices,  $k$  the degree of each vertex,  $\lambda$  the number of common neighbors for adjacent vertices, and  $\mu$  the number of common neighbors for non-adjacent vertices. For instance, in  $N = 16$  vertex graphs,  $G_1$  and  $G_2$  are non-isomorphic but belong to the same family  $(16, 6, 2, 2)$ . The Hilbert space sizes of these graph instances are  $2^{29}$ ,  $2^{100}$ ,  $2^{256}$ , respectively. In this experiment, the three algorithms similarly partition the vertex set based on the degree sequence of the graph and then encode it to generate the system's solution space. Table II presents the detailed structural encoding information of the three graphs, the corresponding number of qubits, the size of the system solution space, and the specific sampling scale per iteration for each algorithm.

As the model parameters converge, the probability amplitude distribution of the quantum system dynamically concentrates towards the low-energy states of the Hamiltonian corresponding to the target problem. Spin configurations that align with lower energy expectations have significantly increased solution probabilities, while those that do not align see a corresponding decrease in solution probability. In particular, the system can only reach the theoretical ground state (with a system energy eigenvalue of 0) when the two graphs are isomorphic. In all non-isomorphic instances, after 100 samples using the NQS algorithm, the experimental ground state energy consistently stabilizes at integer energy levels  $\geq 1$ . This indicates that there are no valid isomorphic mappings in subsequent samples. To mitigate the risk of misjudgment, this algorithm considers a batch of samples valid only when the energy error is 0, ensuring that the mathematical form of the energy expectation is a discrete integer value. This fundamentally eliminates the phenomenon of false convergence, where the energy expectation merely approaches 0.

Fig.7 illustrates the average energy corresponding to the optimal solutions obtained by the three algorithms, indirectly reflecting the quality of solutions achieved after annealing across 100 samples. A lower expected energy intuitively indicates a higher degree of optimization in the spin configuration for vertex mapping, manifesting as an increased proportion of vertex pairs in candidate solutions that satisfy isomorphism constraints. Notably, even

TABLE I. Hyperparameter settings of the three algorithms.

SA	SQA	NQS
$T_0 = 100$	$\Gamma_0 = 100$	learning rate $\in [0.01, 0.1]$
$T_{final} = 0.667$	$\Gamma_{final} = 0.667$	
	Totter slices= 4	

TABLE II. The settings of non-isomorphic parameters.

N	Space Size	Qubits	Sample Size
7	$2^{29}$	29	32
10	$2^{100}$	100	512
16	$2^{256}$	256	2048

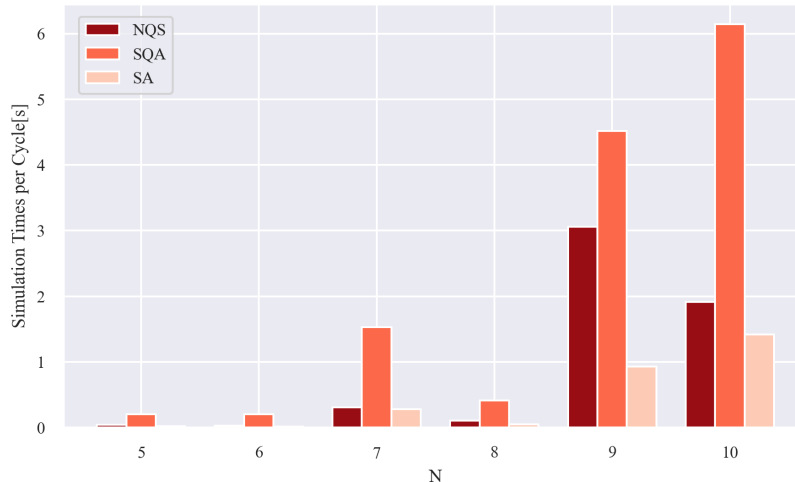


FIG. 10. A comparison chart of the runtime per iteration in seconds for the three algorithms. The NQS algorithm typically maintains a median runtime across all isomorphic graph instances in the experiments, while the runtime of the SA and SQA algorithms lies at the two extremes.

under non-isomorphic conditions, the algorithm can still achieve maximal partial isomorphic coverage. In scenarios involving non-isomorphic graph instances, the NQS algorithm maintains the lowest average energy, outperforming both SQA and SA algorithms.

### C. Isomorphic Graph

We employed a variational method based on NQS to test isomorphic graph instances and verify its ability to correctly distinguish isomorphic graphs. Experiments were conducted on graphs with varying numbers of vertices ( $N = 5, 6, 7, 8, 9, 10$ ) and compared the performance of the NQS method with that of classical SA and SQA. Fig.8 shows the experimental results in graph instances with  $N = 5, 6, 7, 8, 9, 10$  vertices. Both of these annealing algorithms explore the solution space by simulating a gradual cooling process to find the global optimum. Three algorithms partition the vertex set based on the degree sequence of the graph, and then encode and generate the corresponding solution space. The specific graph information, solution space size, the corresponding number of qubits and single sampling size for each algorithm are listed in Table III.

Experimental results show that the NQS method achieves a faster reduction in system energy, converging more quickly to the theoretical minimum. While SA and SQA algorithms control the search direction by lowering the system temperature and transverse field strength, the NQS method accounts for the overall distribution of the system. This enables the NQS method to make more precise adjustments, resulting in a stable and consistent decrease in energy, ultimately maintaining the theoret-

ical global minimum. We observed that, compared to the two annealing algorithms, the initial energy values of the NQS method were higher for some graph instances. This is partly due to the inherent randomness introduced during the sampling step of exploring the solution space. Furthermore, in the NQS method, the energy expectations  $\bar{E}_{loc}$  are calculated after randomly initializing neural network parameters and batch sampling using the M-H sampling method. Unlike SA and SQA algorithms that retain only a single optimal solution vector from batch sampling in the solution space, the NQS method accounts for the overall distribution.

As a result, the energy values computed in the initial iterations of the NQS method tend to be higher, which requires a certain optimization process, but this does not affect the evaluation of the algorithm’s energy reduction speed and stability. The NQS method’s sample estimation process captures a more comprehensive state of the overall system, rather than relying solely on the energy calculation of a single sample. This leads to more precise and effective adjustments to the overall probability distribution of the system, allowing the energy of the system to decrease more rapidly compared to the other two

TABLE III. The settings of isomorphic graph parameters.

N	Degree Sequence	Space Size	Qubits	Sampling Size
5	[2, 2, 2, 2, 2]	$2^{25}$	25	16
6	[1, 2, 2, 3, 2, 2]	$2^{18}$	18	16
7	[3, 3, 3, 3, 3, 3, 6]	$2^{37}$	37	128
8	[5, 4, 5, 4, 3, 2, 1, 4]	$2^{16}$	16	32
9	[8, 8, 8, 8, 8, 8, 8, 8]	$2^{81}$	81	512
10	[7, 7, 8, 8, 7, 8, 8, 8]	$2^{52}$	52	512

algorithms.

To evaluate the algorithm’s performance, we sampled the ground state system after training and calculated the success rate by counting the number of solutions that met the requirements. For comparison, we ran SA and SQA algorithms multiple times and calculated their success rates by counting the number of times the final solutions matched the target solution. Fig.9 shows that our algorithm initially has a lower success rate, but it rapidly increases with more sampling iterations and stabilizes at 1, with lower fluctuations and higher overall hit rates than SA and SQA. Thus, our method, when handling rugged and glassy optimization landscapes, achieves faster sampling and a higher probability of finding the target solution compared to algorithms based on classical simulated annealing principles. While simulated annealing can explore a broader state space by ”hopping” through thermal fluctuations or escaping local minima via simulated quantum tunneling, it cannot alter the sampling probability. Consequently, its sampling dynamics are slower, and the probability of hitting the target solution is lower in complex optimization landscapes.

Meanwhile, we compared the runtime of the three algorithms to complement the difficulty of accurately estimating the complexity of heuristic algorithms. Fig.10 shows that the SA algorithm has the fastest runtime but only moderate success rates, while the SQA algorithm improves accuracy at the cost of significantly increased runtime. The NQS algorithm maintains optimal success rates with runtime falling between the two, within an acceptable range. Additionally, the runtime does not increase with the number of graph vertices, which is related to the problem encoding method. The number of vertices represents only part of the graph information; more complex structures and additional edges often lead to longer convergence times for the algorithm.

## V. CONCLUSIONS

As an emerging approximate quantum system model, NQS has great potential in quantum many-body physics. We encode the graph isomorphism problem as a QUBO problem, map it to the Ising Hamiltonian, and complete the equivalent transformation to the ground state solution of the quantum many-body system. The method was simulated on a classical computer and compared with simulated annealing-based algorithms. In the experimental process, the NQS method uses neural networks to model quantum systems, which is more efficient than traditional annealing formulas. As a result, it provides more accurate estimates when solving for the ground-state energy of the system compared to the SA and SQA algorithms. Moreover, the NQS algorithm replaces the ran-

dom search principle in the solution space of the SA and SQA algorithms with a variational approach. Through the parameterized optimization of the neural network, it can more precisely adjust the distribution of the solution space, thereby more effectively searching for the global optimum, reducing the likelihood of getting trapped in local optima, and improving the accuracy of the algorithm. Although the SA algorithm relies on thermodynamic principles, it is still prone to getting trapped in local optima, the SQA algorithm partially addresses this issue by utilizing the quantum tunneling effect. However, SQA relies on complex computational steps and high resource consumption, which leads to a significant increase in computational time. Therefore, the experimental results fully validate the advantages of the NQS algorithm in terms of both accuracy and efficiency, further demonstrating its effectiveness in solving the graph isomorphism problem.

On this basis, one of our future research directions is to find ways to further reduce the size of the problem solution space. Due to the encoding method, the quantum system corresponding to the correct solution in the problem solution space is often presented in the form of Dicke states. Therefore, we began to think about whether the solution space can be restricted to Dicke state, thereby directly excluding candidate solutions that do not obey the bijective constraints. However, due to the characteristics of the VMC method, even if the initial state is a Dicke state, there is no guarantee that the subsequent state still obeys the Dicke state constraint in the sampling flip operation. Therefore, how to combine Dicke states and variational methods to effectively reduce the size of the solution space needs further research and thinking. In addition, the development of new quantum algorithms, such as quantum neural networks and quantum enhanced optimization methods, will also be an important part of this research direction. These efforts will open up new paths for the future combination of quantum computing and machine learning, thereby achieving breakthrough progress in the field of graph isomorphism problems.

## ACKNOWLEDGMENTS

This research was supported by the National Nature Science Foundation of China (Grants No. 62101600), State Key Lab of Processors, Institute of Computing Technology, CAS under Grant No. CLQ202404, the Beijing Natural Science Foundation (Grant No. 4252006), National Natural Science Foundation of China (Grant No. 62301454), Fundamental Research Funds for the Central Universities (Grant No. SWU-KQ22049), and the Natural Science Foundation of Chongqing, China (Grant No. CSTB2023NSCQ-MSX0739).

---

[1] K. Riesen, Structural pattern recognition with graph edit distance, *Advances in computer vision and pattern recog-*

*nit*ion , 1 (2015).

- [2] A. Merkys, A. Vaitkus, A. Grybauskas, A. Konovalovas, M. Quirós, and S. Gražulis, Graph isomorphism-based algorithm for cross-checking chemical and crystallographic descriptions, *Journal of cheminformatics* **15**, 25 (2023).
- [3] P. Lestrinant, F. Guihéry, and P.-A. Fouque, Automated identification of cryptographic primitives in binary code with data flow graph isomorphism, in *Proceedings of the 10th ACM Symposium on Information, Computer and Communications Security* (2015) pp. 203–214.
- [4] M. Grohe and P. Schweitzer, The graph isomorphism problem, *Communications of the ACM* **63**, 128 (2020).
- [5] L. C. Ray and R. A. Kirsch, Finding chemical records by digital computers, *Science* **126**, 814 (1957).
- [6] R. Mathon, A note on the graph isomorphism counting problem, *Information Processing Letters* **8**, 131 (1979).
- [7] E. M. Luks, Isomorphism of graphs of bounded valence can be tested in polynomial time, *Journal of computer and system sciences* **25**, 42 (1982).
- [8] L. Babai, Graph isomorphism in quasipolynomial time, in *Proceedings of the forty-eighth annual ACM symposium on Theory of Computing* (2016) pp. 684–697.
- [9] D. Conte, P. Foggia, C. Sansone, and M. Vento, Thirty years of graph matching in pattern recognition, *International journal of pattern recognition and artificial intelligence* **18**, 265 (2004).
- [10] B. T. Messmer and H. Bunke, A new algorithm for error-tolerant subgraph isomorphism detection, *IEEE transactions on pattern analysis and machine intelligence* **20**, 493 (1998).
- [11] L. P. Cordella, P. Foggia, C. Sansone, and M. Vento, A (sub) graph isomorphism algorithm for matching large graphs, *IEEE transactions on pattern analysis and machine intelligence* **26**, 1367 (2004).
- [12] L. P. Cordella, P. Foggia, C. Sansone, M. Vento, *et al.*, An improved algorithm for matching large graphs, in *3rd IAPR-TC15 workshop on graph-based representations in pattern recognition* (Citeseer, 2001) pp. 149–159.
- [13] A. Zeguendry, Z. Jarir, and M. Quafafou, Quantum machine learning: A review and case studies, *Entropy* **25**, 287 (2023).
- [14] N. Onizawa, K. Katsuki, D. Shin, W. J. Gross, and T. Hanyu, Fast-converging simulated annealing for ising models based on integral stochastic computing, *IEEE Transactions on Neural Networks and Learning Systems* **34**, 10999 (2022).
- [15] G. Xiutang and Z. Kai, Simulated annealing algorithm for detecting graph isomorphism, *Journal of Systems Engineering and Electronics* **19**, 1047 (2008).
- [16] D. Delahaye, S. Chaimatanan, and M. Mongeau, Simulated annealing: From basics to applications, *Handbook of metaheuristics* , 1 (2019).
- [17] D. Tamascelli and L. Zanetti, A quantum-walk-inspired adiabatic algorithm for solving graph isomorphism problems, *Journal of Physics A: Mathematical and Theoretical* **47**, 325302 (2014).
- [18] J. K. Gamble, M. Friesen, D. Zhou, R. Joynt, and S. Coppersmith, Two-particle quantum walks applied to the graph isomorphism problem, *Physical Review A—Atomic, Molecular, and Optical Physics* **81**, 052313 (2010).
- [19] K. Rudinger, J. K. Gamble, M. Wellons, E. Bach, M. Friesen, R. Joynt, and S. Coppersmith, Noninteracting multiparticle quantum random walks applied to the graph isomorphism problem for strongly regular graphs, *Physical Review A—Atomic, Molecular, and Optical Physics* **86**, 022334 (2012).
- [20] X. Wang, Y. Zhang, K. Lu, X. Wang, and K. Liu, Marking vertices to find graph isomorphism mapping based on continuous-time quantum walk, *Entropy* **20**, 586 (2018).
- [21] Z. Li, Y. Wang, and X. Qiang, A graph isomorphism algorithm based on continuous-time quantum walks, in *2023 2nd International Conference on Computing, Communication, Perception and Quantum Technology (CCPQT)* (IEEE, 2023) pp. 19–24.
- [22] R. H. Warren, Adapting the traveling salesman problem to an adiabatic quantum computer, *Quantum information processing* **12**, 1781 (2013).
- [23] A. Minamisawa, R. Iimura, and T. Kawahara, High-speed sparse ising model on fpga, in *2019 IEEE 62nd International Midwest Symposium on Circuits and Systems (MWSCAS)* (IEEE, 2019) pp. 670–673.
- [24] J. Hertz, A. Krogh, R. G. Palmer, and H. Horner, Introduction to the theory of neural computation (1991).
- [25] X. Qiang, Y. Wang, S. Xue, R. Ge, L. Chen, Y. Liu, A. Huang, X. Fu, P. Xu, T. Yi, *et al.*, Implementing graph-theoretic quantum algorithms on a silicon photonic quantum walk processor, *Science Advances* **7**, eabb8375 (2021).
- [26] Y. Wang, S. Wu, and J. Zou, Quantum annealing with markov chain monte carlo simulations and d-wave quantum computers, *Statistical Science* , 362 (2016).
- [27] F. Gaitan and L. Clark, Graph isomorphism and adiabatic quantum computing, *Physical Review A* **89**, 022342 (2014).
- [28] M. Borowski, P. Gora, K. Karnas, M. Błajda, K. Król, A. Matyjasek, D. Burczyk, M. Szewczyk, and M. Kutwin, New hybrid quantum annealing algorithms for solving vehicle routing problem, in *International Conference on Computational Science* (Springer, 2020) pp. 546–561.
- [29] P. Mills, R. Rundle, J. Samson, S. J. Devitt, T. Tilma, V. Dwyer, and M. J. Everitt, Quantum invariants and the graph isomorphism problem, *Physical Review A* **100**, 052317 (2019).
- [30] K. Brádler, S. Friedland, J. Izaac, N. Killoran, and D. Su, Graph isomorphism and gaussian boson sampling, *Special Matrices* **9**, 166 (2021).
- [31] A. Di Meglio, K. Jansen, I. Tavernelli, C. Alexandrou, S. Arunachalam, C. W. Bauer, K. Borrás, S. Carrazza, A. Crippa, V. Croft, *et al.*, Quantum computing for high-energy physics: State of the art and challenges, *PRX Quantum* **5**, 037001 (2024).
- [32] L. Li and Y. Pan, A fast numerical solver of quantum-inspired ising optimization problems, *arXiv preprint arXiv:2312.05837* (2023).
- [33] E. Crosson and A. W. Harrow, Simulated quantum annealing can be exponentially faster than classical simulated annealing, in *2016 IEEE 57th Annual Symposium on Foundations of Computer Science (FOCS)* (IEEE, 2016) pp. 714–723.
- [34] Y. Bando and H. Nishimori, Simulated quantum annealing as a simulator of nonequilibrium quantum dynamics, *Physical Review A* **104**, 022607 (2021).
- [35] Q.-G. Zeng, X.-P. Cui, B. Liu, Y. Wang, P. Mosharev, and M.-H. Yung, Performance of quantum annealing inspired algorithms for combinatorial optimization problems, *Communications Physics* **7**, 249 (2024).
- [36] V. Vargas-Calderón, N. Parra-A, H. Vinck-Posada, and F. A. González, Many-qudit representation for the travel-



- ling salesman problem optimisation, *Journal of the Physical Society of Japan* **90**, 114002 (2021).
- [37] E. Inack and S. Pilati, Simulated quantum annealing of double-well and multiwell potentials, *Physical Review E* **92**, 053304 (2015).
- [38] R. Martoňák, G. E. Santoro, and E. Tosatti, Quantum annealing by the path-integral monte carlo method: The two-dimensional random ising model, *Physical Review B* **66**, 094203 (2002).
- [39] L. Stella, G. E. Santoro, and E. Tosatti, Monte carlo studies of quantum and classical annealing on a double well, *Physical Review B—Condensed Matter and Materials Physics* **73**, 144302 (2006).
- [40] S. V. Isakov, G. Mazzola, V. N. Smelyanskiy, Z. Jiang, S. Boixo, H. Neven, and M. Troyer, Understanding quantum tunneling through quantum monte carlo simulations, *Physical review letters* **117**, 180402 (2016).
- [41] G. B. Mbeng, L. Privitera, L. Arceci, and G. E. Santoro, Dynamics of simulated quantum annealing in random ising chains, *Physical Review B* **99**, 064201 (2019).
- [42] G. Carleo, I. Cirac, K. Cranmer, L. Daudet, M. Schuld, N. Tishby, L. Vogt-Maranto, and L. Zdeborová, Machine learning and the physical sciences, *Reviews of Modern Physics* **91**, 045002 (2019).
- [43] G. Carleo and M. Troyer, Solving the quantum many-body problem with artificial neural networks, *Science* **355**, 602 (2017).
- [44] Y. Nomura, A. S. Darmawan, Y. Yamaji, and M. Imada, Restricted boltzmann machine learning for solving strongly correlated quantum systems, *Physical Review B* **96**, 205152 (2017).
- [45] G. Torlai, G. Mazzola, J. Carrasquilla, M. Troyer, R. Melko, and G. Carleo, Neural-network quantum state tomography, *Nature physics* **14**, 447 (2018).
- [46] C. S. Calude, M. J. Dinneen, and R. Hua, Qubo formulations for the graph isomorphism problem and related problems, *Theoretical Computer Science* **701**, 54 (2017).
- [47] N. Yoshimura, M. Tawada, S. Tanaka, J. Arai, S. Yagi, H. Uchiyama, and N. Togawa, Mapping induced subgraph isomorphism problems to ising models and its evaluations by an ising machine, *IEICE TRANSACTIONS on Information and Systems* **104**, 481 (2021).
- [48] R. A. Quintero and L. F. Zuluaga, Qubo formulations of combinatorial optimization problems for quantum computing devices, in *Encyclopedia of Optimization* (Springer, 2022) pp. 1–13.
- [49] B. Volkov and Y. V. Kopaev, Contribution to the theory of band ferromagnetism, *Soviet Journal of Experimental and Theoretical Physics Letters* **19**, 104 (1974).
- [50] Z.-A. Jia, B. Yi, R. Zhai, Y.-C. Wu, G.-C. Guo, and G.-P. Guo, Quantum neural network states: A brief review of methods and applications, *Advanced Quantum Technologies* **2**, 1800077 (2019).
- [51] F. Verstraete, Worth the wait, *Nature Physics* **11**, 524 (2015).
- [52] T. J. Osborne, Hamiltonian complexity, *Reports on progress in physics* **75**, 022001 (2012).
- [53] Z.-A. Jia, Y.-H. Zhang, Y.-C. Wu, L. Kong, G.-C. Guo, and G.-P. Guo, Efficient machine-learning representations of a surface code with boundaries, defects, domain walls, and twists, *Physical Review A* **99**, 012307 (2019).
- [54] X. Gao and L.-M. Duan, Efficient representation of quantum many-body states with deep neural networks, *Nature communications* **8**, 662 (2017).
- [55] J. Carrasquilla and R. G. Melko, Machine learning phases of matter, *Nature Physics* **13**, 431 (2017).
- [56] A. Monras, G. Sentís, and P. Wittek, Inductive supervised quantum learning, *Physical review letters* **118**, 190503 (2017).
- [57] V. Dunjko, J. M. Taylor, and H. J. Briegel, Quantum-enhanced machine learning, *Physical review letters* **117**, 130501 (2016).
- [58] N. Zhang, S. Ding, J. Zhang, and Y. Xue, An overview on restricted boltzmann machines, *Neurocomputing* **275**, 1186 (2018).
- [59] G. Torlai and R. G. Melko, Latent space purification via neural density operators, *Physical review letters* **120**, 240503 (2018).
- [60] K. Życzkowski, K. A. Penson, I. Nechita, and B. Collins, Generating random density matrices, *Journal of Mathematical Physics* **52** (2011).
- [61] N. Metropolis, A. W. Rosenbluth, M. N. Rosenbluth, A. H. Teller, and E. Teller, Equation of state calculations by fast computing machines, *The journal of chemical physics* **21**, 1087 (1953).
- [62] C. Gros, Physics of projected wavefunctions, *Annals of Physics* **189**, 53 (1989).
- [63] S. Mohamed, M. Rosca, M. Figurnov, and A. Mnih, Monte carlo gradient estimation in machine learning, *Journal of Machine Learning Research* **21**, 1 (2020).
- [64] M. Herman, E. Bruskin, and B. Berne, On path integral monte carlo simulations, *The Journal of Chemical Physics* **76**, 5150 (1982).